Draft version May 15, 2023
Typeset using LaTeX default style in AASTeX631

# Implementing Radiative Transfer in the Monte-Carlo Method of Simulating Accretion Disks of Supermassive Black Holes

Louis Seyfritz,[1]
UVA Department of Astronomy

[1] *University of Virginia*

## ABSTRACT

We study a new method in simulating the accretion disks of black holes with Athena++, focusing on solving the radiative transfer equation in the main part of the code, inside of the Problem Generator file. After some exposition of our method of computing the geodesics, and our solution to the radiative transfer equation, we will explain our first attempts at the model followed by the resulting intensity plots of supermassive black holes generated by the new version of the simulator, relying less heavily on post-processing. This work considers the case of a thin disk, which has effects on our assumptions of temperature and opacity in the midplane. We will end our study by a discussion of further applications of this implementation to Athena++.

*Keywords:* Supermassive Black hole — Accretion Disk — Athena++ — Radiative Transfer

## 1. INTRODUCTION

Supermassive black holes exist at the centers of most galaxies, with masses ranging from millions to billions of times that of the Sun. One of the most striking features of these black holes is the presence of an accretion disk, a swirling disk of gas and dust that surrounds the object and emits large amounts of radiation.

The radiative transfer process in the accretion disk is a complex phenomenon that involves the absorption, scattering, and emission of radiation by the gas and dust in the disk (Page & Thorne (1974)). As the gas and dust in the disk orbit the black hole, they are subject to intense gravitational forces that cause them to heat up and emit radiation. This radiation is then absorbed and scattered by other particles in the disk, leading to a complex interplay between radiation and matter. Understanding the radiative transfer process is crucial as it provides important clues about the physical processes that are occurring in the disk, as well as the properties of the black hole itself. By studying the radiation emitted by the disk, we can learn about the temperature, density, and composition of the gas and dust in the disk, as well as the mass and spin of the black hole. Furthermore, the radiation emitted by the accretion disk can have a significant impact on the surrounding environment. The intense radiation can ionize the gas in the vicinity of the black hole, leading to the formation of highly energized plasma that can produce powerful jets of particles that stream away from the black hole at nearly the speed of light. These jets can have a profound impact on the surrounding galaxy, influencing the growth of stars and the formation of new planets Dubois et al. (2012). Overall, the radiative transfer process in the accretion disk of supermassive black holes is a complex and fascinating phenomenon that plays a crucial role in shaping the evolution of galaxies and the universe as a whole. Modeling these objects and the interactions that they have with their environments is essential to our understanding of high energy astrophysics.

The goal of our study is to improve the simulations of different models for accretion of black holes. By changing the approach of the Athena++ code that we use for simulations from a post-processing radiation transfer computation (in Python) to more steps in the C++ part of the process, we can start making the radiative transfer more accurate and extensive. It is already being done by other ray-tracing codes for blackholes (RAPTOR, BHOSS...), and can be effectively replicated for Athena++ by Blacklight for instance (White (2022)). However, having all of these tools centralized to Athena++ with no need for post-processing is a powerful asset that we will discuss further throughout this paper.

## 2. METHODS

In this study, we used the radiative transfer code Athena++ to simulate the accretion disks surrounding supermassive black holes. This code solves the equations of hydrodynamics and radiation transport in a general relativistic framework (Davis et al. (2006)).

We represent the radiation field through a discreet number of photon samples. These photon packets are meant to be statistical samples of the radiation field. They have a stochastic random walk through the simulation domain using pseudorandom numbers. The main focus of this project, radiation transfer, is performed by the MonteCarloBlock::TransferPhotons function.

### 2.1. *Photon Class*

The Photon class is used to represent Photon samples, giving every MonteCarloBlock a Photon pointer. The MonteCarloBlock::InitializePhotons function initializes the photon pointer for each photon sample allocated to the process containing the MonteCarloBlock. Before integration, each photon must have an initial position $x^\alpha$, zone indices $i_\alpha$ = ($i_1$,$i_2$,$i_3$) for the right handed triad coordinate system, direction in the local frame k(a), a weight w, absorption coefficient $\alpha_{abs}$, scattering coefficient $\alpha_{scat}$ (to optimize the computation of opacities) and status flag. This status enumeration consists of three options: EVOLVING, ABSORBED, and DESTROYED. The photon sample will stop progressing when its status is set to either ABSORBED, corresponding to physical absorption, or DESTROYED, which is determined by other criteria, such as potential calculation errors.

The photon's direction $k^\alpha$ is initialized in the locally flat frame and then transformed to the coordinate frame at the start of propagation. The temporal component $k^t$ is directly related to the energy of the photon, and the eventual changing of its value describes the gravitational redshift the photon experiences during integration. The weight w represents the number of photons within a given "superphoton" or photon packet and is invariant under frame transformations. This is typically set based on the emissivity of the cell or set to unity. The absorption $\alpha_{abs}$ and scattering $\alpha_{scat}$ coefficients determine how quickly the optical depth $\tau$ decreases to 0.

### 2.2. *Transport and Reference Frames*

In Athena++, the movement of photon samples through the simulation domain is done through the PhotonMover class. This class moves the sample cell-by-cell on straight paths through the domain thanks to a set of photon movers. There are two types of photon movers: the CartesianMover, using Cartesian coordinates in flat spacetime, and the SphericalPolarMover, using spherical polar coordinates in flat spacetime. On the other hand, the GeneralMover class moves the sample through any coordinate system in the MCCoord class by integrating the photon sample using the metric and connection coefficients.

The transport process consists of selecting a distance to the next interaction (scattering/absorption) for each step. Scattering and absorption are evaluated once the photon sample reaches its destination, and the process repeats until the photon sample is either absorbed, destroyed, or escapes the simulation domain. If the sample is still in the domain after a step, it will either be scattered or absorbed or both. If scattering = none in the montecarlo block, then the Photon will be designated absorbed, and its weight will be set to zero. In our code, we provide a FinalizePhoton function, to set any escaped photons to destroyed.

The "boosts" parameter makes the code take the velocity of the cells into account. So photon samples are moved in the coordinate frame, either Eulerian or stationary. The position and layout of the simulation cells are specified in these frames, while scattering and absorption are modeled in the comoving frame. Lorentz boosts or frame transformations to comoving tetrads are then used, accounting for relativistic Doppler shift and aberration. If the scattering is incoherent, opacities are recomputed at the new photon energy, and both the photon sample and opacities are transformed back to the Eulerian or coordinate frame. This results in photon samples that are moving more parallel with the flow having a smaller opacity and a longer mean free path between interaction events, while those moving more perpendicular or antiparallel to the flow velocity have a higher opacity and shorter mean free path.

### 2.3. *Geodesics and Ray Tracing*

In order to get the equation for radiation transfer in an arbitrary spacetime, we need to derive the geodesic equation of a photon, which is used in the ray tracing of our particles. The relativistic radiative transfer part of our simulation

is obtained through ray tracing, a process where rays from photons are traced back in time from the accretion disk to the observer, which we set at our fixed camera in Athena++ (Dexter & Fragile (2011)). Instead of treating a pixel as a single point, the code views a pixel as a square area on the image plane. It samples this area using a ray positioned at its center. As photons reach the accretion flow, we solve the radiative transfer equation, according to the equations that we derive below, along the geodesic. We can then produce images by repeating this process for many rays, with each ray representing a pixel.
The direction of the photon is such that:

$$k^{\alpha} = \frac{dx^{\alpha}}{d\lambda} \tag{1}$$

with $\lambda$ an affine parameter and $x^{\alpha}$ the initial contravariant position components.
In the Hamiltonian form, we consider:

$$\frac{dx^{\alpha}}{d\lambda} = g^{\alpha\beta}k_{\beta} \tag{2}$$

$$\frac{dk_t}{d\lambda} = 0 \tag{3}$$

$$\frac{dk_a}{d\lambda} = -\Gamma^{\alpha}_{\beta\gamma}k^{\beta}k^{\gamma} = -\frac{1}{2}\delta_a g^{\alpha\beta}k_{\alpha}k_{\beta} \tag{4}$$

For g any arbitrary metrics and for no specific coordinate basis. With $\Gamma^{\alpha}_{\beta\gamma}$ the Christoffel symbol, or connection coefficients.
Equation 2.3 is the geodesic equation which determines the change in direction and energy of the photon.
Since our photons are moving in a grid, and being traced back to the observer, we need to compute the geodesics for n+1 iterations, which then takes the form:

$$x^{\alpha}_{n+1} = x^{\alpha}_{n} + k^{\alpha}_{n}\Delta\lambda + \frac{1}{2}\left(\frac{dk^{\alpha}}{d\lambda}\right)_{n}(\Delta\lambda)^2 \tag{5}$$

$$k^{\alpha}_{n+1} = k^{\alpha}_{n} + \frac{1}{2}\left(\left(\frac{dk^{\alpha}}{d\lambda}\right)_{n} + \left(\frac{dk^{\alpha}}{d\lambda}\right)_{n+1}\right)\Delta\lambda \tag{6}$$

$$k^{\alpha}_{n+1,p} = k^{\alpha}_{n} + \left(\frac{dk^{\alpha}}{d\lambda}\right)_{n}\Delta\lambda \tag{7}$$

The stepsize is defined in a grid cell i and by a fractional value $\epsilon$ relating physical size of the grid cell to the wave vector of the photon as:

$$\Delta\lambda = \epsilon\left(\frac{x_{f,max} - x_{f,min}}{k^{\alpha}}\right) \tag{8}$$

With $x_f$ the self−face of each cell and $\epsilon$ determined as an input parameter by the user.
The photon's energy is updated at every step according to:

$$E_{n+1} = E_n\left(\frac{k^{t}_{n+1}}{k^{t}_{n}}\right) \tag{9}$$

The computation of general relativistic correction is also moved to the C++ part of our code. We apply the steady-state disk model as described by Page & Thorne (1974), with a gravity correction and a temperature correction.

### 2.4. *Radiation Transfer Solution*

The first step in solving the radiation transfer equation is to consider the accretion disk of our black hole model as a thin disk emitting blackbody radiation (Jiang et al. (2014) for more model discussion), radiation in thermal equilibrium. The specific intensity of photons, defined as $I_\nu$, is then isotropic. We consider Kirchhoff's Law for thermal emission which tells us that

$$S_\nu = B_\nu(T) = \frac{j_\nu}{\alpha_\nu} \tag{10}$$

Where $j_\nu$ is the emission coefficient for coherent isotropic scattering, $\alpha_\nu$ is the absorption coefficient of the scattering process, also called the scattering coefficient, $B_\nu(T)$ the power absorbed per unit volume and $\nu$ the frequency ranging to the corresponding power emitted.
The equation for unpolarized radiative transfer accounting for general relativity yields:

$$\frac{dI}{d\lambda} = j_\nu - \alpha_\nu I \tag{11}$$

Ignoring polarization effects along rays with the Lorentz invariants and defining $\nu$ as

$$\nu = \frac{\nu_{em}}{\nu_{obs}} \tag{12}$$

We get the intensity and absorption and emission coefficients:

$$I_{obs} = I_{em}\nu^{-3} \tag{13}$$

$$j = j_\nu \nu^{-2} \tag{14}$$

$$\alpha = \alpha_\nu \nu \tag{15}$$

We take j and $\alpha$ to be constant over each ray segment (typically no larger than nearby cells in the simulation).
To determine the emitted intensity, we compute the effective temperature of the radiation, which is determined through the flux, defined as a function of radius, mass, accretion rate but without relativistic and no-torque correction, which are provided by our general relativity correction function. The flux can then be computed according to Shakura & Sunyaev (1973)

$$R_g = \frac{GM}{c^2}, \qquad \dot{m} = \dot{M}/\dot{M}_{edd}, \qquad \dot{M}_{edd} = \frac{4\pi GM}{\kappa_{es}/c} \tag{16}$$

$$F = \frac{3GM\dot{M}}{8\pi R^3} \tag{17}$$

With c the speed of light, G the gravitational constant, $\dot{M}$ the accretion rate of the black hole, $\dot{M}_{edd}$ its Eddington accretion rate, R its radius and $R_g$ its Schwarzschild radius.
We can now calculate the effective temperature, which corresponds to the temperature with a general relativistic correction

$$T_{eff} = (F/\sigma)^{1/4} \times T_{corr} \tag{18}$$

The evolution of I from the start of a cell then employs the well-known exact solution:

$$e_f = e^{\frac{h\nu}{k_b T_{eff}}} \tag{19}$$

$$I_{em} = \frac{2h\nu^3}{c^2(e_f - 1)} \tag{20}$$

With h the Planck constant, $\nu$ the frequency, k the Boltzmann constant and T the temperature. This grants an intensity for every frequency on the grid, making an image for our black hole once given more information from an input file, such as the spin, the mass, the accretion rate of the black hole and the inclination of the camera.

## 3. RESULTS

The solution to the radiative transfer found in Section 2 is only the start of a complete accretion disk model. For better accuracy, multiple iterations of the theory were ran, with a more detailed and complex analysis of the conditions in the disk. We will now go through this part of the theoretical work, followed by an analysis of our results when applied to the code.

### 3.1. *Initial Iterations*

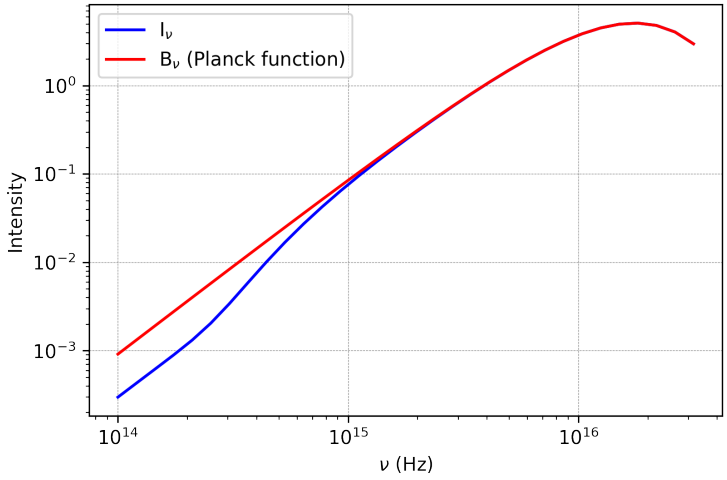


**Figure 1.** Intensity plot comparing the Plank function and the specific intensity on a set range of frequencies

Before implementing code into the already existing simulations in Athena++, we wanted to decide which radiative transfer conditions to implement into our models. For that purpose, multiple iterations were made adding more and more elements to the determination of blackbody radiation, until we reached the equations that we would ultimately input into the Athena++ code.

In accretion disks, it is important to not only consider the blackbody radiation of the disk but also the free−free emission caused by the acceleration of a charge in the Coulomb field of another charge. An interesting aspect of the free−free emission is when we consider it thermally, averaging the single−speed case of electrons over a thermal distribution of velocities. The thermal approach can also be applied to free−free absorption, the absorption of radiation from an electron in the field of an ion.

To compute these processes and relate them to the intensity, we first need to express $B_\nu$ as the Planck's Law:

$$B_\nu(T) = \frac{2h\nu^3/c^2}{e^{\frac{h\nu}{kT}} - 1} \tag{21}$$

The intensity now takes into account the optical depth of the disk and a new definition of the source function (Mihalas & Weibel-Mihalas (1999)):

$$I_\nu = I_0 e^{-\tau_\nu} + S_\nu(1 - e^{-\tau_\nu}) \tag{22}$$

where we defined $\tau_\nu$ as the optical depth such that $\tau_\nu = \Delta\lambda \times \alpha_\nu$, with $\Delta\lambda$ still representing the stepsize, and $S_\nu$ the source function set to

$$S_\nu = \frac{1}{2}\frac{j_\nu^{ff}}{\alpha_\nu^{ff}} \tag{23}$$

Here, $\alpha_\nu^{ff}$ is the free-free absorption coefficient and $j_\nu^{ff}$ the free-free emission coefficient, as respectively defined in equations (5.18b) and (5.14b) of Rybicki & Lightman (1991) where we take $Z = \frac{\rho}{1.67262\times10^{-24}}$

$$\alpha_\nu^{ff} = \frac{dW}{4\pi dV dt d\nu} = 3.7\times10^{-8} Z^2 n_e n_i T^{-1/2}\nu^{-3}(1-e^{\frac{-h\nu}{kT}})(CGS: cm^{-1}) \tag{24}$$

$$j_\nu^{ff} = \frac{dW}{dV dt d\nu} = 6.8\times10^{-38} Z^2 n_e n_i T^{-1/2} e^{\frac{-h\nu}{kT}}(CGS: erg*s^{-1}*cm^{-3}*Hz^{-1}) \tag{25}$$

We would normally need to add the Gaunt factor, $g_{ff}$ (Rybicki & Lightman (1991)) to the equations of these coefficients, but due to the nature of our computations, being in the "Large-angle region" of the formula, and the extent of our study, we consider $g_{ff} \approx 1$

The plot in Figure 1 shows blackbody radiation according to the equations derived above. We observe a slight deviation of the intensity to Planck's function at small intensities, which might be due to our way of defining the opacity, but is insignificant overall. The resulting curves are what we expect our intensity and $B_\nu$ to yield for this range of frequencies.

The code necessary to implement this new part of the theory in Athena++ is still in progress, thus we have yet to run simulations taking into account the Bremsstrahlung part of radiation.

### 3.2. *Black Hole Modeling*

The main results of our efforts are showed in intensity maps of the accretion disk of supermassive black holes, plotted using our updated simulation methods in Athena++. Varying different parameters such as the spin of the black hole and the inclination of the observer, we tested the veracity of our radiative transfer process. The results are shown in Figures 3 and 4.

We set the mass of the supermassive black hole to $10^9 M_\odot$, the accretion rate to 0.1, and the spin to both 0. and 0.9 for an observer with different inclinations. We observe that a Doppler beaming makes the intensity asymmetric from approaching and receding fluid, respectively on the left and on the right. The observer perceives photons emitted from the far side of the accretion flow as positioned above the black hole because of their deflection, and the thick central ring is caused by the gravitational lensing effect of material passing underneath the black hole. There are clear changes between both figures, explained by the difference in spin. The size of a black hole depends inversely on its spin, so a bigger spin grants a smaller black hole. We also observe in Figures 3 and 4, the distribution of intensities around the black hole, which depend on the distance from the singularity. The gas closest to the event horizon has the highest intensity, with the Doppler beaming effect making it more prevalent on the left side, as mentioned prior.

Figure 2 is a comparison of the post-processing, or old simulation, method of determining the radiation transfer of the accretion disk (on the left) to the new method with the radiation transfer in the C part of the code directly in Athena++ (on the right). The resolution is improved, with 64 by 64 pixels images, allowing us to compare the images with more accuracy. The simulations are not exactly the same, we observe a slight extension of the event horizon on the left of the black hole in our new method, as well as a smoother top part for this inclination. However, they are similar enough to show that our change in methods was successful in making an almost identical model in a more effective and flexible way.

## 4. SUMMARY

Rather than solving the transfer equation in post-processing, which limits the variables that we can modify and thus the overall usefulness of our simulations, we produced a model directly in the Athena++ Problem Generator, making it possible to apply some general relativistic modifications to the radiative transfer directly, with $T_{eff}$ corrected in any coordinate frames for instance.

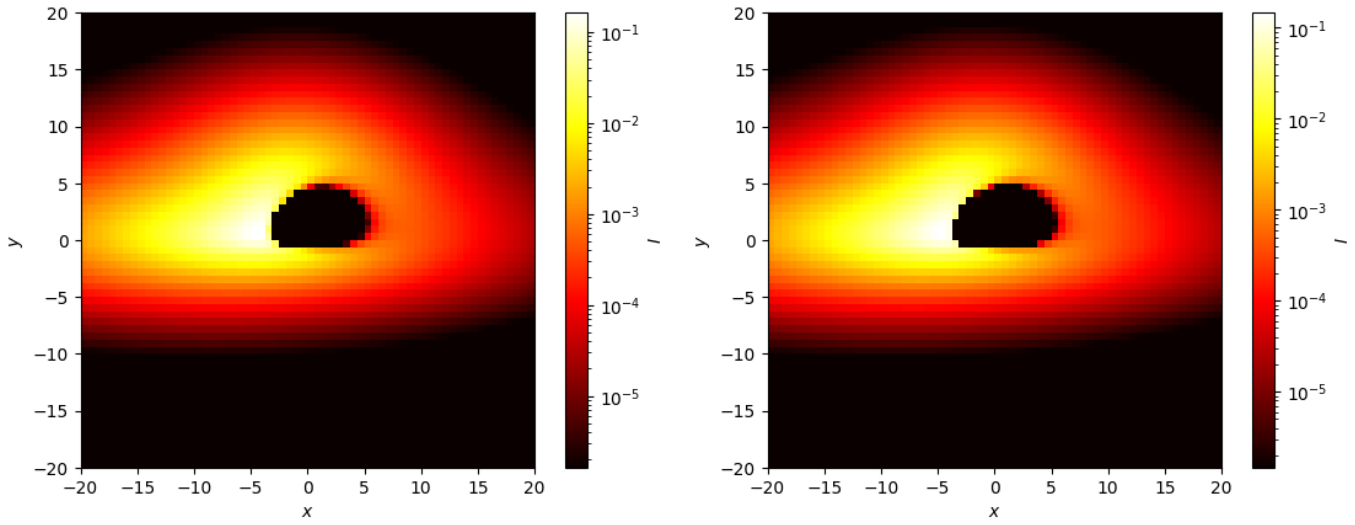


(a) (b)

**Figure 2.** Intensity plot of accretion disk of supermassive black hole with M = $1 * 10^9 M_\odot$, $\dot{M} = 0.1$, spin a = 0.9 and at an inclination of 75° for a 64 by 64 pixels grid comparing the old simulation method (left) and the new method (right)

### 4.1. *Future Implementations*

Now that the radiative transfer part of the code lies in Athena++, our next step will be to start combining the integration of the intensity in order to add free emission and absorption to the model. By integrating directly through the cells, we can stop treating the accretion disk that we model as a thin disk. Our integration currently goes to the midplane, but with this new piece of code, it becomes possible to go further and integrate the path of photons through a thick disk and back, considering opacity (Abramowicz & Fragile (2013)). The ray tracing of Athena++ is adaptive, based on mesh refinement, and to fully exploit the capabilities of the code, the accretion disk needs to have a thickness. With a depth to the disk, photons can pass through the midplane and give back information on its composition and nature. Some will be marked as destroyed, when passing into the event horizon, but most will reach the outer radius of the disk, on the other side of the black hole, and be integrated backwards to our camera. The temperature and $\rho$ currently have to be fed to the code as inputs in the Problem Generator, which is something that needs to be changed as the temperature should evolve through the grid as well as the density.
The code is ready for its next steps in numerical simulations, with our ability to now take snapshots from simulations through the simulation grid.

### 4.2. *Conclusion*

After solving the radiative transfer equation analytically in Python and applying our findings to the processing part of the simulation code for black holes in Athena++, we were able to make one of the first fully functional simulator of black holes inside of Athena++ with no need for post-processing.
In this thesis, we first established the functioning of our simulations, using the Athena++ code to create photons in a grid and, after setting a coordinate frame, move the photons as packets or "superphoton" through cells. Since supermassive black holes are highly relativistic objects, we derived the geodesics of the photons and the way our Monte Carlo process can ray trace them to a fixed observer. We then provided a solution for the radiative transfer for our model of accretion disk and presented a more complete solution considering free-free emission and absorption that will be implemented in our main code in the future. The models created with our new method were then presented and explained, since they show good agreement with both our older models and the literature (White (2022)), our work seems to have been successful. Finally, we covered the future of this research, with the next steps in implementations for our simulations, with the goals to make the model as accurate as possible and Prof. Shane Davis as happy as possible as well.

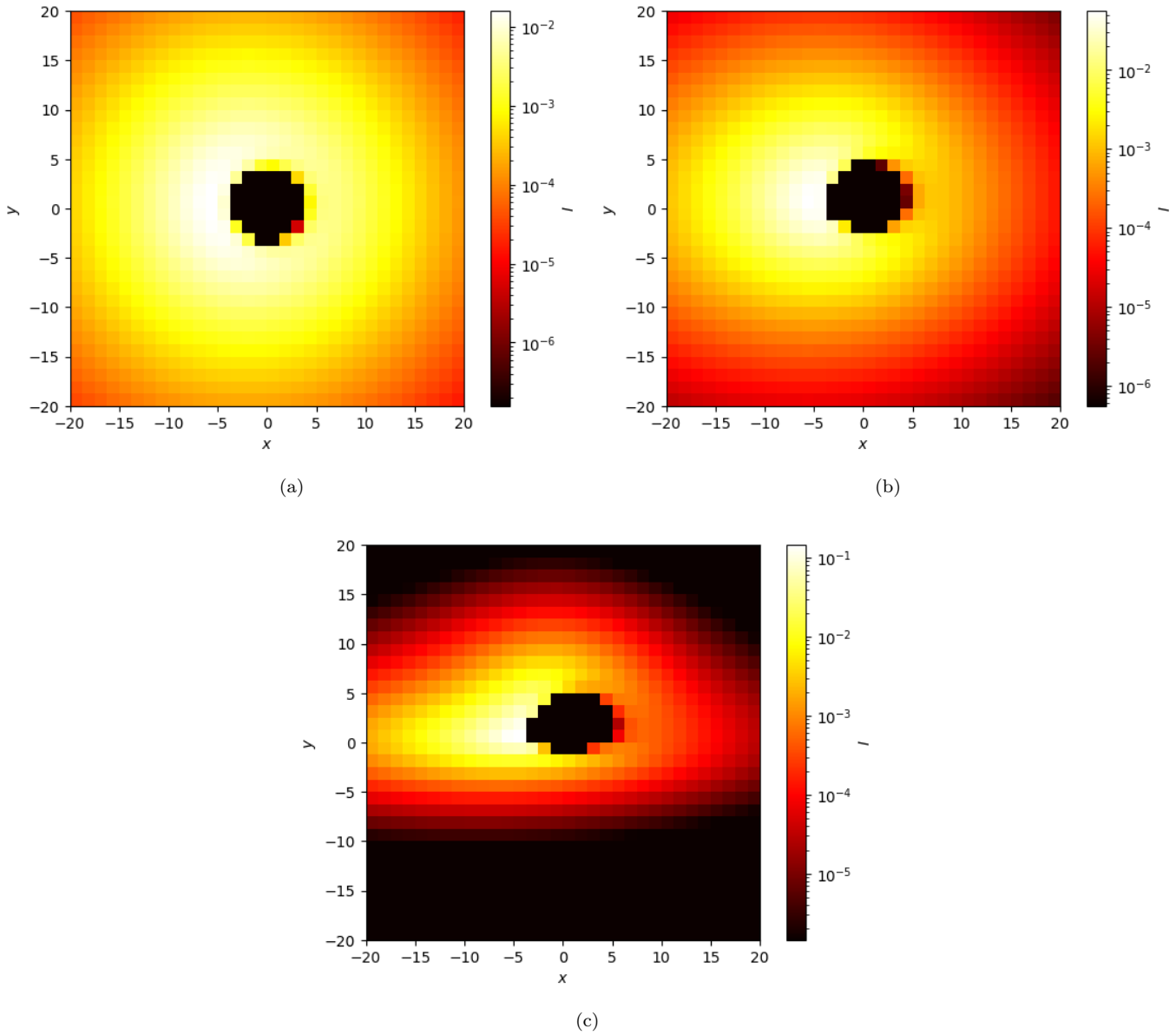


**Figure 3.** Intensity plot of accretion disk of supermassive black hole with M = $1 * 10^9 M_\odot$, $\dot{M} = 0.1$, spin a = 0.9 and at an inclination of 15° for (a), 45° for (b) and 75° for (c) (32 by 32 pixels)

I want to thank Professor Shane Davis, my advisor who made this project possible and supported me through it, as well as my peers and friends in the astronomy department. We are a small but strong and dedicated group of students! Je voudrais aussi remercier ma famille; mes parents, toujours là pour moi, et mon frère, qui trouve toujours un moyen de me faire sourire. Merci maman, merci papa, merci Victor!

## REFERENCES

Abramowicz, M. A., & Fragile, P. C. 2013, Living Reviews in Relativity, 16, 1

Davis, S. W., Done, C., & Blaes, O. M. 2006, The Astrophysical Journal, 647, 15

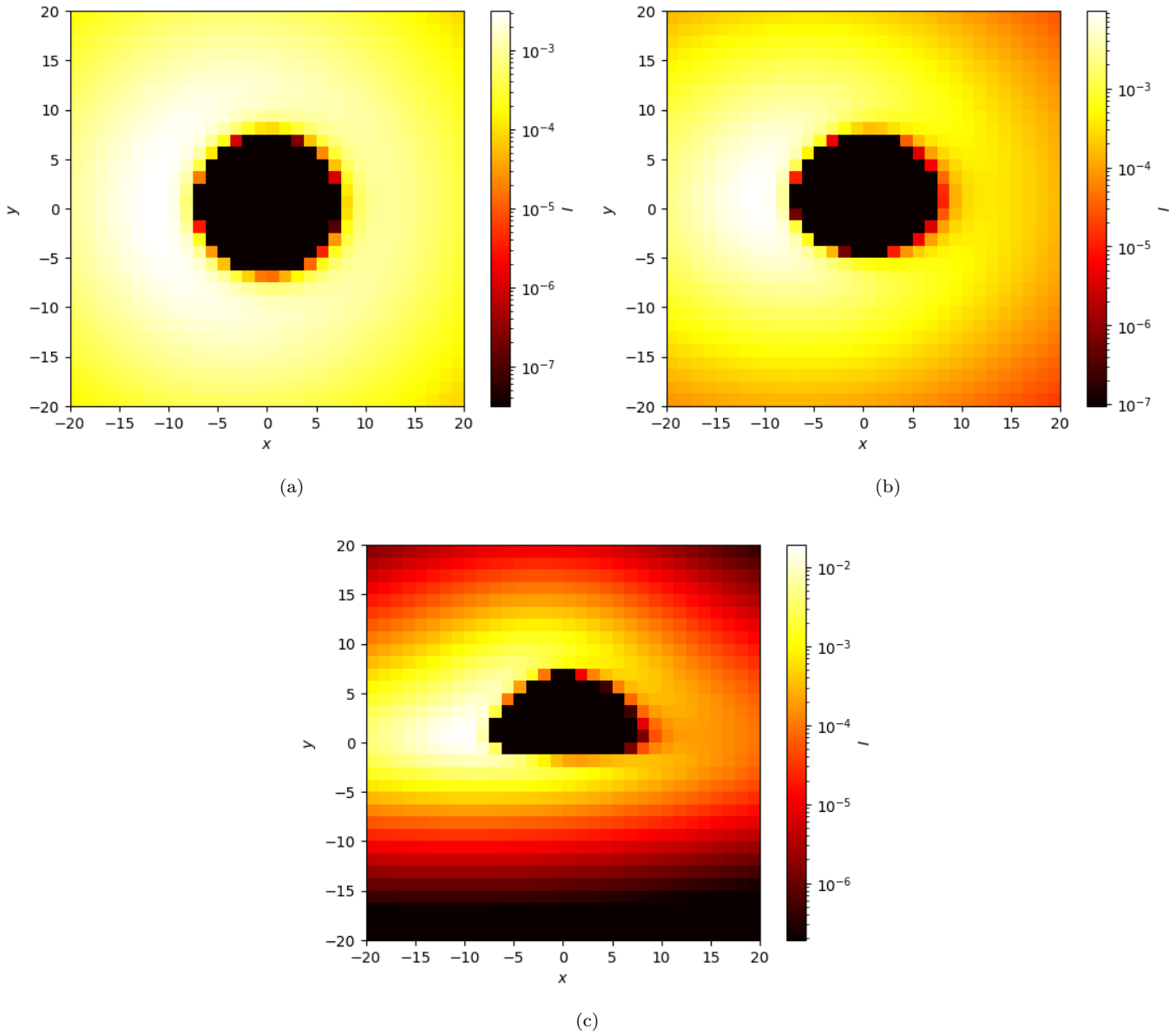


**Figure 4.** Intensity plot of accretion disk of supermassive black hole with M = $1 * 10^9 M_\odot$, $\dot{M} = 0.1$, spin a = 0. and at an inclination of 15° for (a), 45° for (b) and 75° for (c) (32 by 32 pixels)


Dexter, J., & Fragile, P. C. 2011, The Astrophysical Journal, 730, 36, doi: 10.1088/0004-637X/730/1/36

Dubois, Y., Devriendt, J., Slyz, A., & Teyssier, R. 2012, Monthly Notices of the Royal Astronomical Society, 420, 2662

Jiang, Y.-F., Stone, J. M., & Davis, S. W. 2014, The Astrophysical Journal, 796, 106, doi: 10.1088/0004-637X/796/2/106

Mihalas, D., & Weibel-Mihalas, B. 1999, Foundations of radiation hydrodynamics (Courier Corporation)

Page, D. N., & Thorne, K. S. 1974, The Astrophysical Journal, 191, 499

Rybicki, G. B., & Lightman, A. P. 1991, Radiative processes in astrophysics (John Wiley & Sons)

Shakura, N. I., & Sunyaev, R. A. 1973, Astronomy and Astrophysics, 24, 337

White, C. J. 2022, The Astrophysical Journal Supplement Series, 262, 28, doi: 10.3847/1538-4365/ac77ef